Postprint of: Manshari S., Koziel S., Leifsson L. Compact Dual-Polarized Corrugated Horn Antenna for Satellite Communications, IEEE Transactions on Antennas and Propagation (2020) DOI: 10.1109/TAP.2020.2980337

Compact Dual-Polarized Corrugated Horn Antenna for Satellite Communications

Saeed Manshari, Slawomir Koziel, *Senior Member, IEEE*, and Leifur Leifsson

***Abstract*—In this paper, a structure and design procedure of a novel compact dual-polarized corrugated horn antenna with high gain and a stable phase center for satellite communication is presented. The antenna incorporates an Ortho-Mode Transducer (OMT), a mode converter, and a corrugated structure. The compact OMT section is designed to be fed by standard WR-75 waveguides. The proposed compact design utilizes only ten corrugated slots to yield a symmetric radiation pattern. The antenna impedance bandwidth (VSWR < 1.5) is 10.2 GHz to 15 GHz. Furthermore, the antenna exhibits 14 dBi to 17 dBi gain, a constant 30-degree HPBW radiation pattern, and less than 9mm phase center variation over the operating frequency range. The aperture diameter is 7 cm and the total antenna length is 15 cm. Due to the aforementioned features, the proposed antenna is suitable as the feed reflector for both uplink and downlink satellite communication. The design is validated numerically and experimentally.**

***Index Terms*—Antenna radiation patterns, horn antennas, phase center, OMT.**

I. Introduction

In recent years, reflector antennas have been widely utilized to provide high gain as required by the link budget equation in satellite communications. The satellite systems can be divided into military and commercial ones. The commercial satellites use 10.95 GHz to 12.5 GHz range for a downlink and 14 GHz to 14.5 GHz range for an uplink [1-2]. To reduce the space and the ground stations size, utilization of the same antenna for both the uplink and downlink has been advocated. Typically, the commercial satellite systems employ the vertical and horizontal linear polarizations. Consequently, the dual polarized antennas covering the desired frequency ranges are needed. For applications that require two polarizations, the employment of either the inherently dual polarized quad-ridged horns or single polarized antenna combined with an ortho-mode transducer (OMT) have been proposed [1-3].

Simultaneous coverage of the uplink and downlink ranges can be realized with coaxial-type multi-band horn antennas that resonate in multiple bands, or by using wideband horn antennas covering the mentioned ranges. However, the manufacturing process of the coaxial-type horn antennas is complex and expensive. Furthermore, as the aforementioned antennas are single polarized, application of the OMTs is necessary. Passive three-port OMTs consist of two independent ports and a common port. The independent ports are coupled to the common port and isolated from each other. These ports carry the orthogonal modes TE_{10} and TE_{01} which provide the vertical and horizontal polarizations propagation, respectively [4-6]. Since the commercial OMTs are narrowband, individual OMT should be used for each frequency band. This results in bulky feeding structures [2]. From the point of view of satellite applications, one of the most important characteristics of OMTs is port isolation. The OMTs can be categorized into three groups, two-fold, one fold and, asymmetric OMTs. Although the two-fold structures ensure wideband operation, they are bulky and complex, therefore expensive in fabrication [5-9]. On the other hand, asymmetric OMTs are compact, however, their operating band is restricted. As an example, the three-port asymmetric OMT for the X-band applications has been recently presented [10]. It provides 45 dB port isolation but the operating bandwidth is only 11.5 % [10]. Among these three configurations, the one-fold OMT provides relatively broad operating band, compact design, and high isolation [5], [9]. Conventional one-fold OMTs can provide up to 30 dB isolation. Recently, by tapering the waveguide width, 45 dB port isolation has been achieved [8]. Unfortunately, apart from the considerable length of the OMT of [8], its other deficiency is that the independent ports cover the narrow 13.75 GHz to 14.5GHz and 10.95 GHz to 12.5 GHz bands, respectively, therefore, both ports cannot be simultaneously used for uplink and downlink channels.

Utilization of OMTs can be avoided by the employment of dual-polarized horn antennas such as quad ridged ones. Over the recent decade, the profiled dual-polarized wideband horn antennas have been widely applied as feed reflectors [11-14]. However, these antennas exhibit constant beamwidth over the wide frequency range, a high cross-polarization level, and unsymmetrical radiation pattern [11-14]. On the other hand, corrugated horn antennas provide high gain, low sidelobe level, low cross polarization level, and rotational radiation patterns which are desirable characteristics for reflector feeds [15-37]. To attain the aforementioned features, the hybrid HE_{11} mode should be excited on the aperture. The corrugations on the side wall of the horn excite and support the HE_{11} mode in the flare of the horn antenna. As the feed section of these antennas are circular waveguides for which the fundamental modes are TE_{11}, between three to seven transition slots are required. The depth of the transition slots varies from $\lambda/2$ to $\lambda/4$; this transition keeps the input reflection at the acceptance level. As the commonly used corrugated horns usually require at least fifteen slots, they exhibit a considerable length, large size and weight [15-37]. Moreover, a large number of slots contributes to the increased price and the fabrication complexity of the antenna. As a way of overcoming this

Manuscript was submitted on July 2, 2019. This work was supported in part by the Icelandic Centre for Research (RANNIS) Grant 174573051, and by the National Science Centre of Poland Grant 2015/17/B/ST6/01857.

S. Manshari and S. Koziel are with Engineering Optimization and Modeling Center of Reykjavik University, Reykjavik, Iceland (e-mails: saeedm@ru.is, koziel@ru.is); L. Leifsson is with Department of Aerospace Engineering, Iowa State University, IA, USA (e-mail: leifur@iastate.edu). S. Koziel is also with the Faculty of Electronics, Telecommunications and Informatics, Gdansk University of Technology, Gdansk, Poland.

This article has been accepted for publication in a future issue of this journal, but has not been fully edited. Content may change prior to final publication. Citation information: DOI 10.1109/TAP.2020.2980337, IEEE Transactions on Antennas and Propagation

issue, a hybrid ridged and four-slot corrugated wideband horn antenna has been introduced [38]. This antenna provides constant 10-dB beamwidth and the constant phase center over the X and Ku bands, but it is an inherently single polarized structure [38].

In this article, a novel compact dual polarized corrugated horn antenna operating within the 10.2 GHz to 15 GHz bandwidth is presented. The novelty of the design is the use of a compact multi-step and wideband OMT combined with an only ten-slot corrugated horn antenna. The proposed OMT structure ensures a relatively broad operating range at the Ku band and provides isolation better than 45 dB. As the corrugated horn feed is a circular waveguide, the structure is also equipped with a short-length TE_{10}-to-TE_{11} mode converter. Moreover, in the proposed design, the slot depth variation over the ten slots is only 0.1λ. This does not only reduce the antenna diameter but it also facilitates the milling process and reduces the overall structure weight. As the first slot performs as a half-wave transformer and the antenna diameter relates to the slot depth, to reduce the slot depth without affecting the antenna performance, the first slot in the corrugated horn is filled with teflon. These characteristics, among others, the number of slots, polarization, operating frequency, feed section, and employed matching techniques, indicate significant differences between the proposed OMT and the one of [38]

The proposed antenna yields a constant half power beam width (HPBW), constant phase center, the rotational pattern for two polarization and low cross polarization level over the operating frequency range. The overall length of the antenna structure with the OMT section is 15 cm (6 cm without OMT) and the aperture diameter is 7 cm. As for practical applications, each independent OMT port is designed to be fed by a WR75 waveguide, the wideband (10 GHz to 15 GHz) WR75-to-coaxial adaptor has been designed and fabricated for the testing purposes.

II. Design Procedure

This section describes the geometry and design procedure of the proposed antenna. Its block diagram and topology have been shown in Figs. 1(a) and 1(b), respectively. The structure comprises three sections: the OMT section, the mode converter, and the ten-slot corrugated horn. Further, Fig. 2, presents the design flowchart.

A. The OMT Design and Parametric Studies

The proposed OMT employs a one-fold symmetry configuration with two stepped arms and T-junction structure using an E-plane 90-degree bend. Providing the degenerate TE_{10} and TE_{01} modes on the common port of the OMT for the entire operating band is the main objective at the first stage. At the same time, the higher order modes (e.g., TE_{11} and TM_{11}) should be suppressed, which poses a size limitation on the waveguide dimension. According to the aforementioned limits and target operating band, the independent axial (vertical) and lateral (horizontal) ports are chosen to be WR75, whereas the dimension of the common port is set to 19.8 × 19.8 mm^2. Figure 1 shows these ports as ports 1, 2, and 3, respectively. The multi-step rectangular waveguide transition for both the vertical and the horizontal ports provides the matching section of the OMT. As illustrated in Fig. 1(a), the width W and the height H of the waveguide are changed at each discontinuity step to suppress excitation of the undesirable higher-order modes while keeping VSWR and isolation below the acceptable level. On the other hand, upon passing discontinuities, evanescent higher-order modes are excited, which do not propagate. However, because of storing the reactive energy, they can be used as an imaginary element of the matching network. Hence, the step length L is utilized to improve the feed matching. To calculate the effect of the steps on the input impedance, the modal expansion and the Mode Matching Method (MMM) can be used [4]. Excitation of the higher-order modes and the decay of the evanescent modes both depend on the dimension of the transition steps (height, width, and length).

In this study as shown in Fig.3, the smooth WR75 to a square waveguide with the multi-step transition have applied for two polarization routes. Moreover, in the proposed design, for each OMT arm, a five-step waveguide transition has been used with discontinuities symmetrical in both directions.

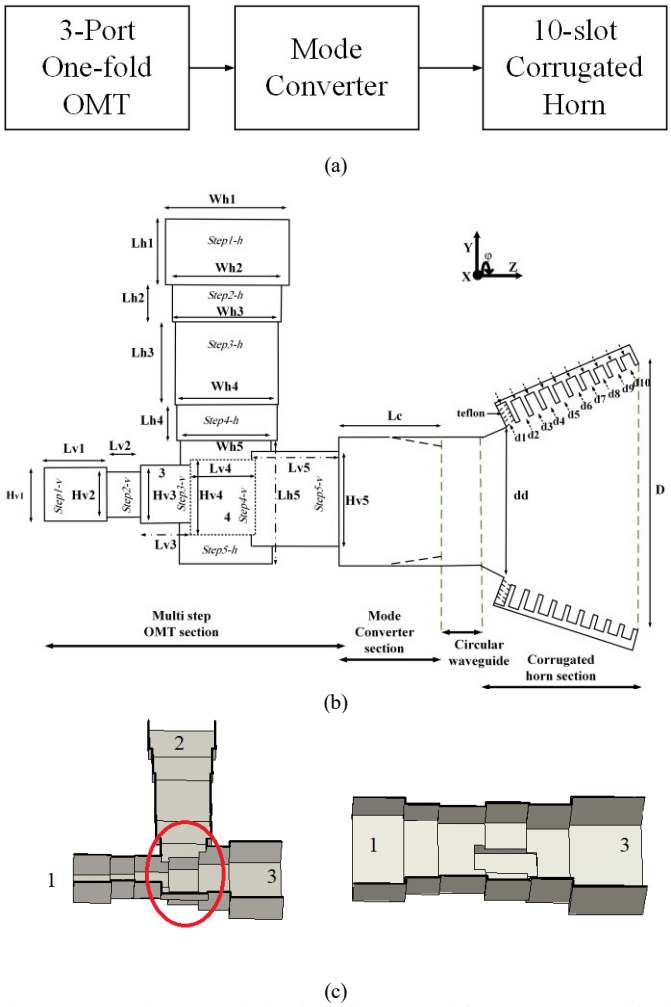

Fig. 1. Proposed compact dual-polarized corrugated horn antenna: (a) block diagram, (b) side view, (c) perspective side view (right) and top view (left) of the OMT structure. The relevant antenna dimensions are presented in Table I. The symbols H, L, W, v, and h stand for the height, length, width, vertical and horizontal polarizations, respectively.

This article has been accepted for publication in a future issue of this journal, but has not been fully edited. Content may change prior to final publication. Citation information: DOI 10.1109/TAP.2020.2980337, IEEE Transactions on Antennas and Propagation

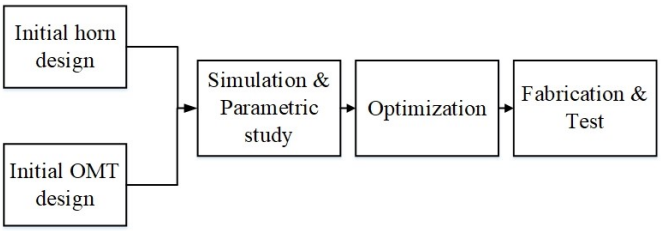

Fig. 2. Flowchart of the antenna design stages.

The intersection of the two arms (the OMT core) is allocated within the fourth step of the straight arm (horizontal polarization route) and the fifth step of the perpendicular arm (vertical polarization route). The OMT core and the E-plane bend have been shown in Fig. 1(c). This section diverts the horizontal polarization into the lateral waveguide. At the intersection step, the width and the height of the vertical waveguide become the height and the width of the horizontal waveguide, respectively. To prevent the degenerate mode excitation in the other route, the height of the main route (or the width of the other route) should be less than the half-wavelength cutoff.

TABLE I OPTIMIZED DIMENSIONS OF THE PROPOSED ANTENNA

Parameter	L_{h1}	L_{h2}	L_{h3}	L_{h4}	L_{h5}	L_{v1}	L_{v2}	L_{v3}	L_{v4}	L_{v5}	L_c
Value [mm]	10	9.1	15.4	8.4	19.7	10.5	6.9	9.6	8.6	8.8	14.9
Parameter	d_1	d_2	d_3	d_4	d_5	d_6	d_7	d_8	d_9	d_{10}	D
Value [mm]	8.5	8.3	7.9	7.6	7.2	6.8	6.4	6	5.7	5.4	55.6
Parameter	W_{h1}	W_{h2}	W_{h3}	W_{h4}	W_{h5}	H_{h1}	H_{h2}	H_{h3}	H_{h4}	H_{h5}	L_w
Value [mm]	19.05	16.9	15.8	15.5	12.8	9.75	8	6.8	5.7	5.5	11.8
Parameter	H_{v1}	H_{v2}	H_{v3}	H_{v4}	H_{v5}	W_{v1}	W_{v2}	W_{v3}	W_{v4}	W_{v5}	dd
Value [mm]	9.75	8.2	9.1	12	16.1	19.05	16.3	15.4	17	16.4	24.1

In the initial design, by considering the aforementioned notes, the height, width and the length of each step are to be designed to provide the smooth and compact transition through the standard dimension ports to the square port within the operating band. The dimensions of each step are obtained through the parametric study and numerical optimization where the primary objective is a reduction of the reflection at each port while keeping the port isolation over 45 dB, and maintaining the compact size of the antenna. The obtained values are presented in Table I.

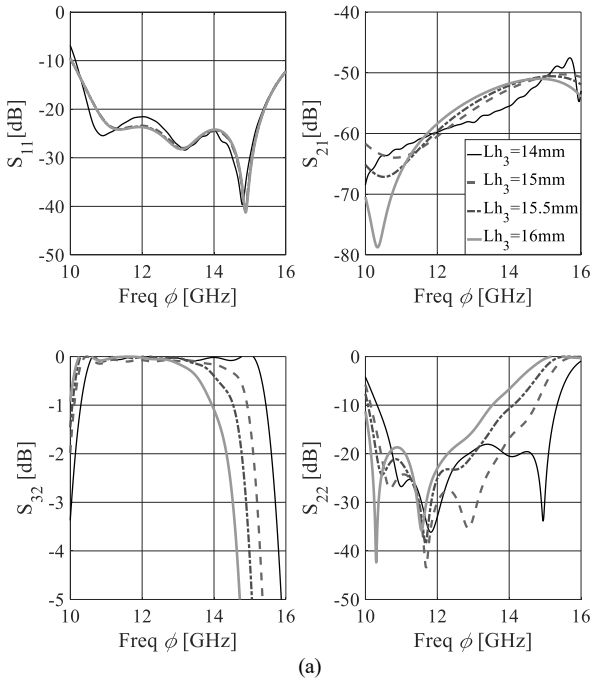

(a)

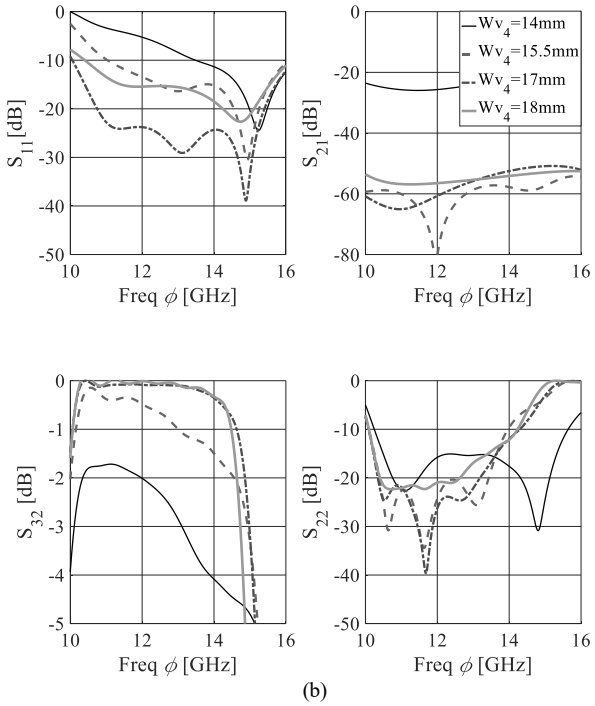

(b)

This article has been accepted for publication in a future issue of this journal, but has not been fully edited. Content may change prior to final publication. Citation information: DOI 10.1109/TAP.2020.2980337, IEEE Transactions on Antennas and Propagation

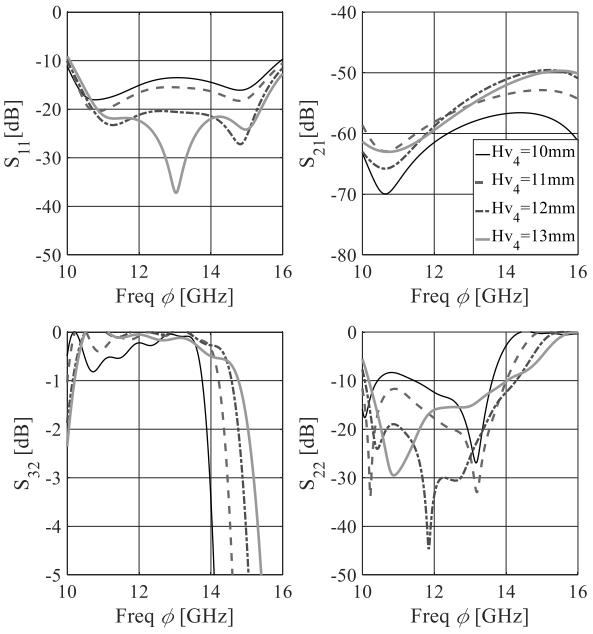

(c)

Fig. 3. Parameter study on the critical OMT parameters. S_{11}, S_{22}, S_{32} S_{21} represent, respectively, the input reflection at Port1 and Port 2, horizontal route insertion loss and isolation between the two independent ports.

Due to a large number of parameters, in this section, only the results of the parametric study on the parameters L_{h3}, H_{v4}, and W_{v4}, are presented. In these studies, one parameter is swept and the remaining parameters are fixed at the values of Table I. Figure 3(a) demonstrates the impact of the variation of the third step length of the horizontal route (L_{h3}) on the reflection of the horizontal port and isolation between the ports. Further, the impact of the sweep parameter of the intersection dimension on the reflection ports, isolation and insertion loss are demonstrated in Figs. 3(b) and 3(c). It can be observed, the best isolation, port reflection and insertion loss within the target operating band are indeed obtained for the parameter values of Table I.

Table II shows a comparison between the main characteristics of the designed OMT and the recent one fold-OMTs designs from the literature.

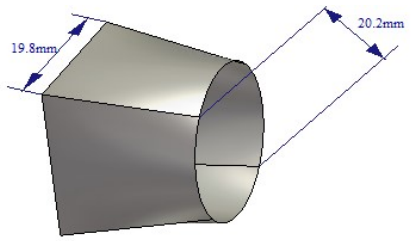

Fig. 4. Mode converter and its relevant dimensions.

B. Mode converter and Corrugated horn Design

As the corrugated horn structure is conical, the compact TE_{10} (or TE_{01}) to TE_{11} mode converter has been used in the overall design. As shown in Fig. 4, the mode converter provides the smooth transition with 19.5 mm length (L_C), from a square section of 28 mm diameter to a circular section of 20 mm diameter. This diameter supports the circular waveguide fundamental mode in the operating band.

The opening angle of the horn and the depth of the first slot are the two important parameters that influence the input reflection of the corrugated horn. The novelty of the proposed design is the utilization of only ten slot corrugations with a relative smooth depth transition on the internal sidewall of the antenna which provides the hybrid HE_{11} mode within the entire operating band. In the corrugated horns, when the hybrid modes are excited, both of the longitudinal fields (E_z and H_z) are nonzero, whereas the tangential fields, E_φ and H_φ are zero. In order to excite the hybrid mode, the anisotropic boundary conditions should be ensured. The corrugation on the internal wall of the horn section creates an anisotropic impedance surface. This leads to the longitudinal and the transversal impedances becoming infinitive and zero, respectively.

Excitation of the HE_{11} hybrid mode requires the depth of the slot to be λ/4. On the other hand, to reduce the input reflection, the depth of the first slot in the common corrugated horn design should be λ/2. For smooth transition between λ/2 and λ/4, utilization of a large number of slots is unavoidable. As the first slot performs similarly to the half-wavelength impedance convertor, by filling it with the dielectric, the propagation constant increases therefore, the length of the impedance converter could be decreased. Further, in the proposed design, the length of the first slot is 0.33λ. Owing to this, only 0.1λ depth variation needs to be realized over the series of ten slots. The value of the rests slots is obtained through optimization.

TABLE II COMPARISON WITH STATE-OF-THE- ONE- FOLD OMT DESIGNS

Design	Operation Freq (GHz)	Coverage of Ports	Bandwidth ratio(%)	Dimension (L×H)	Isolation
[5]	10.9-14.5	Simultaneously both Pol.	28	$2.88\lambda_o \times 1.78\lambda_o$	35
[6]	35-44	Simultaneously both Pol.	22	$5.3\lambda_o \times 1.25\lambda_o$	35
[7]	17-22 31-27	V H	13 25	–	40
[8]	10.95-12.5 13.75-14.5	H V	13 5	$2.85\lambda_o \times 1.8\lambda_o$	–
[9]	17.5-20.5	Simultaneously both Pol.	15	$6.15\lambda_o \times 1.6\lambda_o$	30
This work	10.2-15	Simultaneously both Pol.	38	$2.4\lambda_o \times 2.6\lambda_o$	45

This article has been accepted for publication in a future issue of this journal, but has not been fully edited. Content may change prior to final publication. Citation information: DOI 10.1109/TAP.2020.2980337, IEEE Transactions on Antennas and Propagation

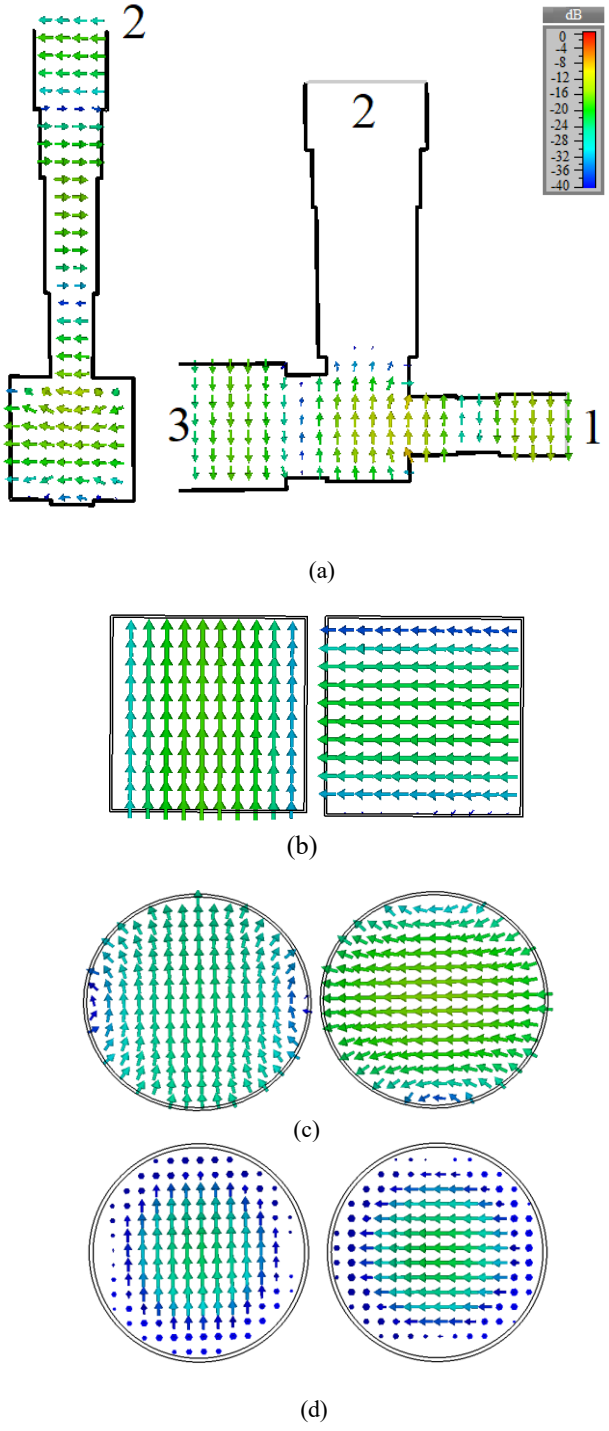

Fig. 5. Electrical field distribution for two polarizations: (a) side section on the both arms and the square waveguide (b) TE_{10} and TE_{01} modes field pattern on the square OMT port, (c) TE_{11} mode field pattern for two polarizations on the output port of mode converter, (d) HE_{11} mode field pattern for two polarizations on the aperture of the antenna.

The last few slots operate as resonators and generate the hybrid HE_{11} mode on the horn aperture. To avoid excitation of the higher order modes in the slots, the slot width should be less than half of the minimum wavelength of operation. The ratio of the teeth width to the slot width is another important parameter which influences the cross polarization level. The proposed structure features a relatively compact corrugation section which decreases the antenna complexity and its fabrication costs. Moreover, the semi angle of the proposed design is 17-degree which provide the 30-degree HPBW over the operation band.

Finally, the electric field patterns for the two polarization routes on various cross-sections are presented in Fig. 5. The figure depicts the mode conversion from the rectangular waveguides through the corrugated flare.

C. WR75 to Coaxial Adapter Design

For practical applications, both the vertical and horizontal ports are designed to be fed by the standard WR75 waveguide. However, for certain purposes (including the measurement procedures) feeding through coaxial cables is necessary. In such cases, the waveguide-to-coaxial adapter is required.

Commercially available adaptors are bulky and expensive and their insertion loss is relatively high. Here, a dedicated low-loss and compact WR75-to-coaxial adaptor for the frequency range of 10 GHz to 15 GHz has been designed (cf. Fig.6)). The adaptor dimensions have been tuned by means of numerical optimization.

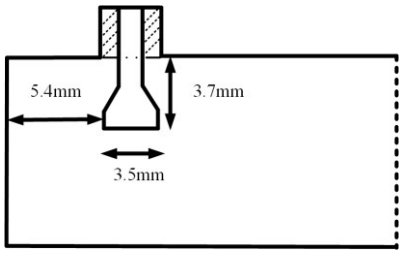

Fig. 6. Cross side of the wideband coaxial to WR-75 adaptor

III. Simulation and Measurement Results

The antenna performance is evaluated using CST Microwave Studio, also used for parameter tuning. The simulation results indicate that the proposed OMT and mode converter design satisfy the specifications for both high mode conversion efficiency and high port isolation. As mentioned in the previous sections, the hybrid HE_{11} distribution on the aperture provides the rotational radiation pattern. The simulated pattern of the propsed antenna is illustrated in Fig. 7.

The variation of the feed phase center over the operating band is another parameter that affects the reflector antenna efficiency in satellite communication. The allocation of the phase center (APC) from the aperture for two polarizations is presented in Table III. This variation for the proposed design is less than 9 mm over the operating band. To further validate the design, the antenna and two WR75-to-coaxial converters have been fabricated using the milling process with the CNC machine and the 50μm mechanical tolerance. Figure 8 shows the prototype antenna and the WR75 to coaxial adaptors. The VSWR was measured by the HP8510 network analyzer and the radiation pattern was extracted in the anechoic chamber. As indicated in Fig. 9, the simulated and measured VSWR is below 1.5 over the operating band. Figure 10 shows the simulated and measured patterns on the E and H planes. It can be observed that the

This article has been accepted for publication in a future issue of this journal, but has not been fully edited. Content may change prior to final publication. Citation information: DOI 10.1109/TAP.2020.2980337, IEEE Transactions on Antennas and Propagation

agreement between the simulation and measurement within the 20 dB beamwidth is very close. Slight differences between the simulations and measurements are a result of the mechanical tolerances in the fabrication and the assembly process. As it can be seen in Fig. 11, the cross-polarization level is below 45 dB.

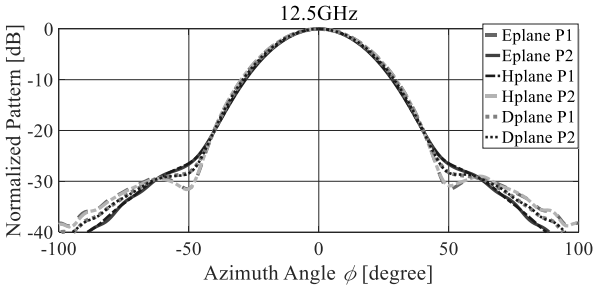

Fig. 7. The radiation pattern for two polarizations in E-plane (φ=90), H-plane (φ=0) and D-plane(φ=45).

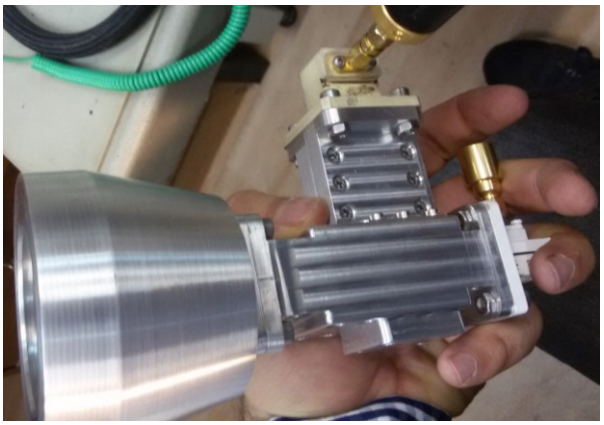

Fig. 8. Photograph of the fabricated dual polarized horn antenna prototype.

TABLE III THE ALLOCATION OF PHASE CENTER FROM THE APERTURE*

Freq. [GHz]	11^{p1}	11^{p2}	11.5^{p1}	11.5^{p2}	12^{p1}	12^{p2}	12.5^{p1}	12.5^{p2}	13^{p1}
APC [mm]	3.5	3.5	4.6	4.7	5.1	5.1	5.7	5.7	7.2
Freq. [GHz]	13^{p2}	13.5^{p1}	13.5^{p2}	14^{p1}	14^{p2}	14.5^{p1}	14.5^{p2}	15^{p1}	15^{p2}
APC [mm]	7.3	7.4	7.4	8.4	8.4	10.7	10.7	12.3	12.2

* p1 and p2 stand for vertical and horizontal polarization, respectively.

TABLE IV MEASURED PHASE CENTER

Frequency [GHz]	11	11.5	12	12.5	13	13.5	14	14.5	15
APC [mm]	3.8	4.8	5.2	6	6.8	7.2	8.4	9.8	12.5

The peak gain of the horn is depicted in Fig. 12. It varies from 14 dB to 17.2 dB across the 10.5 GHz to 15 GHz frequency band. Moreover, the aperture efficiency of the antenna is more than 80%.

Because the measurement results of the phase center location for two polarizations over the operating band are similar, in Table IV, the results for only one polarization are presented. The test setup is similar to that used in [27]. For the phase center measurement, the maximum variation of 0.5 degrees in over the angular range of -20 to +20 degrees has been considered. The obtained result is well matched with Table III. Moreover, Table V illustrates a comparison between the main characteristics of the proposed antenna and the recent corrugated and ridged feed horn antenna designs from the literature. It can be observed that the presented design offers the most competitive combination of performance figures, including compactness with dual-polarization capability, phase center stability, aperture efficiency, and low cross polarization. Although the length of the proposed antenna as presented in Table V does not include the OMT, the overall length of the antenna-OMT system is still short compared to the previous works such as [22]. Furthermore, when compared to other antennas featuring comparable length, the proposed design exhibits better cross-polarization and aperture efficiency.

Although ridge horn antennas provide relatively large bandwidth, their radiation pattern is not symmetric. Moreover, their cross-polarization level is high. These two deficiencies create serious issues for satellite feed reflector antennas.

TABLE V COMPARISON WITH STATE-OF-THE-ART HORN DESIGNS

Design	Bandwidth ratio (f_{max}/f_{min})	Length (λ_{fmin})	Polarization	Antenna type	Phase center variation	Cross Polar (dB)	Aperture efficiency %
[12]	6:1	1.1	Dual	Ridged	5cm	–8	50-70
[13]	6:1	1.07	Dual	Ridged	3cm	–10	50-60
[14]	5.2:1	2	Dual	Ridged	-	–12	60-78
[20]	2.25:1	2	Single	Corrugated	-	-	20-50
[21]	1.67:1	8.05	Single	Corrugated	-	–35	60
[22]	1.16:1	10 (no OMT)	Dual	Corrugated	-	–40	-
[23]	1.26:1	4.4	Single	Corrugated	-	–57 (sim)	-
[24]	1.6:1	4	Single	Corrugated	-	–20	50-80
[25]	1.1:1	0.3	Single	Corrugated	-	–25	60-73
[38]	3.3:1	2.6	Single	Hybrid	4cm	-20	53-76
[39]	3:1	3.2	Single	Ridged	3cm	-	48-77
[40]	3:1	3.5	Single	Ridged	3.5cm	-	44-67
This work	1.5:1	2 (no OMT)	Dual	Corrugated	9mm	–40	80-87

This article has been accepted for publication in a future issue of this journal, but has not been fully edited. Content may change prior to final publication. Citation information: DOI 10.1109/TAP.2020.2980337, IEEE Transactions on Antennas and Propagation

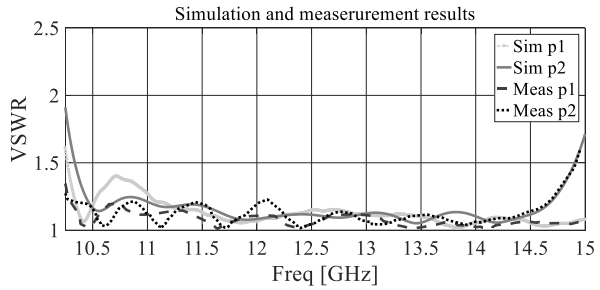

Fig. 9. Simulated and measured VSWR of the proposed design.

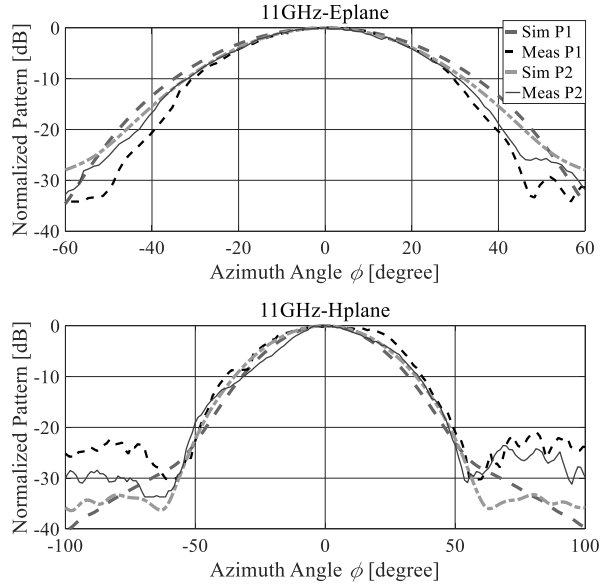

(a)

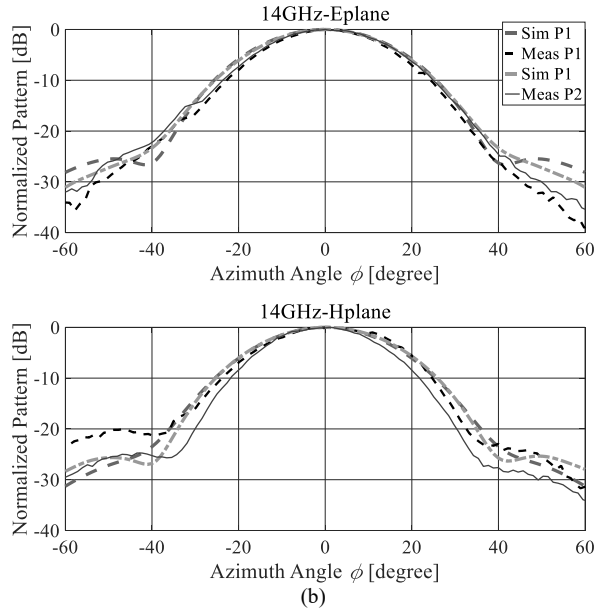

(b)

Fig. 10. Simulated and measured radiation pattern of two polarizations on the E-plane and H-plane: (a) 11 GHz, (b) 14 GHz.

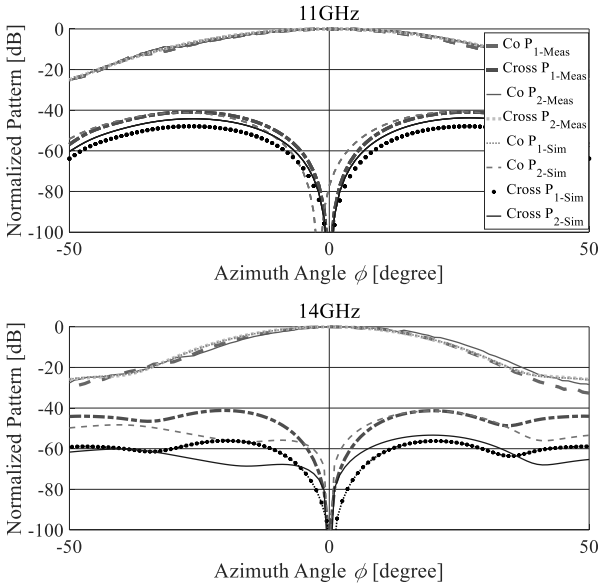

Fig. 11. Measured co- and cross-polarization of two ports on the *D*-plane.

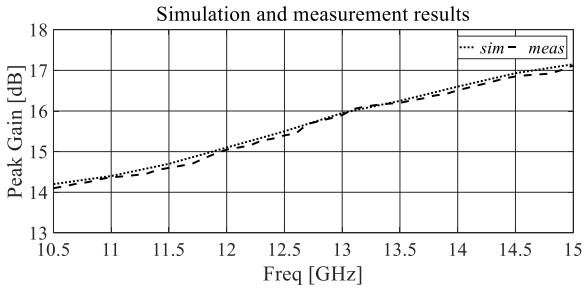

Fig. 12. Simulated and measured radiation pattern of two polarizations on the E-plane and H-plane: (a) 11 GHz, (b) 14 GHz.

IV. Conclusion

In this letter, a novel compact dual-polarized corrugated feed horn antenna for commercial satellite communication has been proposed. The impedance bandwidth for two polarizations (VSWR < 1.5) is 10.2 GHz to 15 GHz. The variation of the phase center is less than 9 mm within the operating band. Furthermore, the proposed design exhibits a symmetrical rotational pattern with the constant 30-degree, HPBW radiation pattern for two polarization over the operating band. The proposed design benefits from the novel compact OMT structure that provides the port isolation better than 45 dB. The experimental results indicated good agreement between the simulated and measured characteristics of proposed antenna.

The major advantages of the design, apart from its excellent electrical and field performance, include compactness, as well as easy and low-cost manufacturing process. The latter results from a simpler structure (fewer corrugations) as compared to the previously reported designs. Further, the aperture diameter is 7 cm and the total antenna length with the OMT is 15 cm. The achieved characteristics make the antenna suitable to work as the feed reflector for the satellite and astronomy communications, all of which need high gain, dual-polarized

and constant phase center antennas. One of the objectives of the future work will be the development of compact OMT featuring isolation acceptable for practical applications.

REFERENCES

[1] Zhang, P., Qi, J., & Qiu, J. "Efficient design of axially corrugated coaxial-type multi-band horns for reflector antennas". *Int. J. Microw. Wireless Tech.*., vol. 9, no. 10, pp. 1975-1981, 2017.

[2] S. D. Targonski, "Design of a X/Ku multiband feed antenna for satellite communications", in *Proc. 2015 IEEE Int. Symp. Antennas Propag.*, 2015, pp. 1040-1041.

[3] S.D. Targonski, "A multiband antenna for satellite communications on the move", *IEEE Trans. Ant. Prop.,* vol. 54, no. 10, pp. 2862-2868, Oct. 2006.

[4] A. M. Boifot "Classification of ortho-mode transducers", *Eur. Trans. Telecommun.,* vol.2, no.5, pp. 503-510, 1991.

[5] J. A. Ruiz-Cruz, J. R. Montejo-Garai, and J. M. Rebollar, "Optimal configurations for integrated antenna feeders with linear dual-polarisation and multiple frequency bands," *IET Microw., Antennas Propag.,* vol. 5, no. 8, pp. 1016–1022, Jun. 2011.

[6] X. Shang, P. Klasmann, and M. J. Lancaster, ''A compact Ka-band waveguide orthomode transducer fabricated by 3-D printing,'' in Proc. *Eur. Microw. Conf.,* London, U.K., Oct. 2016, pp. 365–368.

[7] Yanfei Li, "A simple waveguide OMT designed for millimeter wave applications," in Proc. *Microw and Milliw Techn., (ICMMT) 2016 IEEE International Conference*, Beijin, China, Jun. 2016, pp. 576 - 578.

[8] P.K. Verma, R. Kumar " Realization of Ku-Band ortho-mode transducer with high port to port isolation" *Prog. Electromagn. Res.Lett.*, vol. 74, pp. 111-115, 2018.

[9] M. A. Abdelaal, S. I. Shams, M. Moharam, A. Mahmoud and A. Kishk, "Compact full band OMT based on double-mode double ridged waveguides", *IEEE Trans. Microw. Theory Techn.,* vol. 66, no. 4, pp.1856-1863, Apr. 2018.

[10] M. A. Abdelaal, S. S. Ahmed, and A. Kishk, "Asymmetric compact OMT for X-Band SAR applications", *IEEE Trans. Microw. Theory Techn.,* vol. 66, no. 4, pp.1856-1863, Apr. 2018.

[11] O.B. Jacobs, J.W. Odendaal, and J. Joubert, "Quad-ridge horn antenna with elliptically shaped sidewalls", *IEEE Trans. Ant. Prop.*, vol. 61, no. 6, pp. 2948-2955, Jun. 2013.

[12] A. Akgiray, S.A. Weinreb, W. Imbriale, and C. Beaudoin, "Circular quadruple-ridged flared horn achieving near-constant beamwidth over multioctave bandwidth: design and measurements", *IEEE Trans. Ant. Prop.*, vol. 61, no 3, pp. 1099-1108, Mar. 2013.

[13] T.S. Beukman, P. Meyer, V. Ivasgina, and R. Maaskant, "Modal-based design of a wideband quadruple-ridged flared horn antenna" *IEEE Trans. Ant. Prop.*, vol. 64, no 5, pp. 1615-1625, May 2016.

[14] B. Dong, J Yang, J. Dahlastrom, J. Flygare, M. Pantaleev, and B. Billade, "Optimization and realization of quadruple-ridged flared horn with new spline-defined profiles as a high-efficiency feed from 4.6 GHz to 24 GHz", *IEEE Trans. Ant. Prop.*, vol. 67, no. 1, pp. 585-590, Jan. 2019.

[15] P. J. B. Clarricoats, "Analysis of spherical hybrid modes in a corrugated conical horn", *Electron. Lett*., vol. 5, pp. 189-190, May. 1969.

[16] P. J. B. Clarricoats and A. D. Olver, *Corrugated Horns for Microwave Antennas*, London, IEE, 1984.

[17] C. Granet and G. L. James, "Design of corrugated horns: A Primer," *IEEE Antennas Propag. Mag.*, vol. 47, pp. 76-84, Apr. 2005.

[18] G. L. James, "Design of wide-band compact corrugated horn," *IEEE Trans. Ant. Prop.*, vol. 32, pp. 1134-1138, Oct. 1984.

[19] X. Zhang, "Design of conical corrugated feed horns for wide-band high-frequency applications," *IEEE Trans. Microw. Theory Tech.* vol. 41, pp. 1263-1274, Aug. 1993.

[20] M. Abbas-Azimi, F. Mazloumi, and F. Behnia, "Design of broadband constant-beamwidth conical corrugated-horn antenna," *IEEE Antennas Propag. Mag.*, vol. 51, no. 5, pp. 109-114, Oct. 2009.

[21] J. Teniente, A. Martínez, B. Larumbe, A. Ibáñez, and R. Gonzalo, "Design guidelines of horn antennas that combine horizontal and vertical corrugations for satellite communications", *IEEE Trans. Ant. Prop.*, vol. 63, no. 4, pp. 1314-1323, Apr. 2015.

[22] R.C Gupta, M. B Mahajan and R Jyoi, "Compact high-gain composite horn antenna for space-borne beacon application" ", *Int. J. El. Lett.* vol. 106, no.2, pp.305-317, Oct. 2018.

[23] F. Li, G. Liu, L. Wang, E. A. Balfour, J. Wang, Y. Pu, and Y. Luo, "Design and microwave measurement of a Ka-band HE11 mode corrugated horn for the Faraday rotator", *IET Microw. Antennas Propag.* vol. 11, pp. 75, Jan. 2017.

[24] J-C.S. Chieh, B. Dick, S. Loui, and J.D. Rockway "Development of a Ku-band corrugated conical horn using 3-D print technology", *IEEE Antennas Wireless Propag. Lett.*, vol. 13, pp. 201-204, Jan. 2014.

[25] H.C. Moy-Li, D. Sánchez-Escuderos, E. Antonino-Daviu, and M. Ferrando-Bataller, "Low-profile radially corrugated horn antenna", *IEEE Antennas Wireless Propag. Lett.*, vol. 16, pp. 3180-3183, Oct. 2017.

[26] Z. Frank, "Very Wideband Corrugated Horns," *El. Lett.,*vol.11, pp. 131-133, Mar.1975.

[27] A. D. Olver and J. Xiang, "Design of Profiled Corrugated Horns," *IEEE Trans. Ant. Prop.*, vol. AP-36, pp. 936-940, July 1988.

[28] J. Teniente, R. Gonzalo, and C. Rio, "Ultra-Wide Band Corrugated Gaussian Profiled Hom Antenna Design," *Antennas Wireless Propag. Lett.*, vol. 12, pp. 20-21, Jan. 2002.

[29] R. Gonzalo, J. Teniente, and C. Rio, "Improved Radiation Pattern Performance of Gaussian Profiled Hom Antennas," *IEEE Trans. Ant. Prop.*, vol. AP-50 ,pp.1505-1513, Nov. 2002.

[30] J. Teniente, R. Gonzalo, and C. Rio, "Innovative High-Gain Corrugated Hom Antenna Combining Horizontal and Vertical Corrugations," *Antennas Wireless Propag. Lett.*,vol.5, pp. 380-383, 2006.

[31] B. M. Thomas, "Design of Corrugated Conical Horns," ," *IEEE Trans. Ant. Prop.*, vol.AP-26, pp.367-372, Mar. 1978.

[32] A. Densmore, Y. Rahmat-Samii, G.Seck, "Corrugated-Conical Horn Analysis Using Aperture Field With Quadratic Phase", *IEEE Trans. Ant. Prop.*, vol. 59, no. 9, pp. 3453-3457, 2011.

[33] R.J. Wylde, D.H. Martin, "Gaussian beam-mode analysis and phase-centers of corrugated feed horns *IEEE Trans. Microw. Theory Techn.,* vol. 41, no. 10, pp. 1691-1699, 1993.

[34] K.S. Rao, "A simple dual-band corrugated horn with low cross polarization", *IEEE Trans. Ant. Prop.*, vol. 38, no. 6, pp. 946-951, 1990.

[35] Z. Ni, H. Shi, T. Zhang, X. Zhao, J. Li and N.Xia, "A ku-band dual polarized corrugated horn" in Proc. *2018 Intern. Conf. on Electronic. Tech. (ICET),*pp.147-158, 2018.

[36] Xiaoyu Du, Shufeng Zheng, Huidong Li, Zhao Zhou, Zhaohui Wei, Yingzeng Yin, Yuanming Cai, Xin Xue, "A Compact KU/E Band Horn Antenna", in Proc. *Asia-Pac. Microw. Conf. (APMC),* pp. 1609-1611, 2018.

[37] Stefano Maddio, Renzo Nesti, Giuseppe Pelosi, Monica Righini, Stefano Selleri, "Profiled Corrugated Horn for Compact and High Efficiency Feeds", in Proc. *Intern. Conf. on Electromag. Advac. App. (ICEAA)* International Conference on, pp. 675-678, 2018.

[38] S. Manshari, S. Koziel and L. Leifsson, "A wideband corrugated ridged horn antenna with enhanced gain and stable phase center" *Antennas Wireless Propag. Lett.*, vol. 18, pp. 1031-1035, May. 2019.

[39] S. Manshari, F. Hodjat-Kashani, G. Moradi, and M. Sarijlo "The comparison of two structures of wide band horn antenna", *Int. J. El. Lett.*, available online, Mar. 2018.

[40] S. Manshari, F Hodjat-hashani, G. Moradi, M. Sarijlo "A novel two-step flare wide band horn antenna" *Microw. Opt. Tech. Lett*. vol. 60, no. 2, pp. 283-289, Jan. 2018. L. Kerr and M. J. Timochko, Broadband Corrugated Horn with Double-Ridged Circular Waveguide, US Patent 4,021,814, May 3,1977.